Penerbit Akademia Baru

Journal of Advanced Research in Fluid Mechanics and Thermal Sciences

Journal homepage: www.akademiabaru.com/arfmts.html
ISSN: 2289-7879

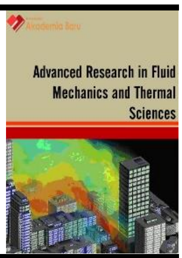

Two-Dimensional CFD Simulation Coupled with 6DOF Solver for analyzing Operating Process of Free Piston Stirling Engine

Open Access

Alliche Ridha[1], Announ Mohamed[1,*], Chetti Boualem[2], Kermezli Tayeb[1]

[1] Laboratory LME, Medea University, 26000 Ain D'heb Medea, Algeria
[2] Laboratory of Industrial Fluids, Measurements and Applications, University of Djilali Bounaama- Khemis Miliana, Aindefla, Algeria

ARTICLE INFO

Article history:
Received 15 December 2018
Received in revised form 19 February 2019
Accepted 22 February 2019
Available online 10 March 2019

Keywords:
Free piston Stirling engine, ANSYS Fluent, fluid-structure interactions, 6DOF solver, static and dynamic state

ABSTRACT

This work focuses on developing a two-dimensional axisymmetric simulation of the entire free piston Stirling engine (FPSE) using ANSYS Fluent to evaluate its output power. The engine model used in this study is the Sunpower B-10B which is thoroughly investigated in different conditions including static and dynamic state. A six-degree-of-freedom (6DOF) solver is used for the first time in this study to solve the problem of fluid-structure interactions between the working gas and the rigid-bodies (Piston and displacer) and therefore enabling to determine accurately the piston and displacer amplitudes as well as the frequency and phase difference under the engine's operating conditions.

1. Introduction

Around the globe, a tremendous number of people are living in very remote and rural areas where access to electricity is very complex due to the lack of power networks whose installation is excessively costly. Therefore, to meet these people's need for electricity, the Stirling engine can be used as an environmentally-friendly solution because it converts renewable energies such as solar energy, biogas and biomass into electricity [1,2]. Moreover, this engine has proven to be as efficient as Carnot engine [3,4].

The Stirling engines fall into two types, the kinematic and the dynamic [5]. The Kinematic engine is easier to investigate compared to the later one because the piston and the displacer are connected to each other. This makes it possible to know their amplitudes as well as the difference phase. Alpha, beta and gamma Stirling engines are considered as kinematic engines. In the dynamic engine both the piston and displacer are free to move independently and their motions are coupled through the working fluid pressure which makes this type of engine more advantageous than the kinematic engine due to its simple structure [6], and the absence of the connecting rod which solves the

[*] *Corresponding author.*
E-mail address: moh_announ@yahoo.fr (Announ Mohamed)

lubrication problem of the rotary shaft as well as the sealing system involved in order to make it possible to use lighter gases such as helium or hydrogen to obtain very high power [7]. Moreover, it can operate over a long period of time without any maintenance [8,9]. However, the analysis of this type of engine is more complicated due to the disconnection between the piston and the displacer. The free piston Stirling engine (FPSE) investigated in this study is known as dynamic engine.

Extensive research has been conducted to examine a Stirling engine using various analysis methods which fall into four categories [10].

Zeroth Order Analysis is an empirical approach based on several experimental data identified by William Beale to determine the power output [11]. However, it is not effective enough in yielding accurate results.

Unlike the Zeroth Order, the First Order Analysis is an analytical approach proposed by Gustav Schmidt in 1871 who considers both the compression and expansion spaces to be isothermal. The temperature of the working fluid is not only the same as that of the hot source in the expansion space but it is also similar to that of the cold source in the compression space knowing that the heat exchange appears to be perfect. In addition, the fluid pressure in the engine is assumed to be uniform whereas the kinetic and potential energies of the gas are not taken into consideration, and the variation of volumes in the cylinder seems to be sinusoidal [12]. Although the performance of Stirling engine is overestimated in this model because of the unrealistic assumptions mentioned previously [13,14], it remains better than the Zero Order. Moreover in 1960 Finkelstein suggested a more realistic model called adiabatic analysis, he considered both the compression and expansion spaces to be adiabatic rather than isothermal [15]. In spite of that, the performance of Stirling engine remains overestimated due to all the thermal and mechanical losses occurring in the engine which are not taken into account in this type of analysis [16].

The accuracy is improved by introducing the Second Order Analysis which integrates the various power losses such as the thermal losses (the imperfect heat transfer in the exchangers, regenerator imperfections, heat conduction from the hot parts to the cold parts) and the energy losses as a result of the shuttle effect which occurs due to the motion of piston, the pumping losses and the drop in pressure resulting from the viscous friction of gas during the fluid flow in the different parts of the engine [17]. The obtained results are much more realistic compared with those obtained based on the First Order Analysis. Some recent works done by Cheng and Yu [18], Mehdizadeh and Stouffs [19] have adopted this approach.

On the other hand, the Third Order Analysis (one-dimensional analysis) which enhances the accuracy of the models by dividing the space in the engine into multiple control volumes and nodes under the operating conditions of engine including the temperature and pressure. The conservation equations of mass, momentum, and energy in addition to the gas state equation are applied to each control volume where an empirical formula for friction coefficient and heat transfer coefficient are used. Numerical methods have been applied to solve the equation system governing the process [17]. It is worth noting that this model is defective because it doesn’t properly simulate the fluid flow, particularly the turbulence, and it uses the empirical correlations to calculate the heat transfer and friction coefficients which seems to be inadequate to obtain accurate results. Some of the analyses at this level were developed by Urielli [20], Finkelstein [21], Tew *et al.,* [22], Organ [23], and Gedeon [24].

Finally, the Fourth Order Analysis (multi-dimensional) has recently been developed by using CFD codes (Computational Fluid Dynamic). Regardless of the different geometries of the engine, this model carries out a finer analysis of the different types of flows and physical phenomena occurring (turbulence, viscous friction, etc.) when the working gas flows back and forth between the two spaces (compression and expansion). many attempts to apply this type of analysis on Stirling engines has been performed focused on separated components of the engine. There have been very limited numbers of works studying the full cycle. Mahkamov [25] has developed an axisymmetric CFD approach using the standard k-ε turbulence model for compressible flow to analyze the working process of V-type solar Stirling engine. The results of this approach were compared with those obtained using the Second Order Analysis under the same operating conditions. The engine output power were found to be over estimated by 250%. A 3D CFD approach was applied on the gamma biomass Stirling engine by Mahkamov [26]. The same engine was also analyzed by using the First Order and Second Order approaches. The comparison to the experimental data conducted under the same conditions showed that the results of the First Order is far less than the expected ones, and the accuracy of the Second Order is about 30%, while for the 3D CFD model it is between 12-18 %. Li *et al.,* [27] presented a three-dimensional CFD study using Fluent to investigated the effects of porous-sheets heat exchangers on the performance of a small scale alpha type Stirling engine. They validated this study with both the experimental data and the analytical solution. A CFD simulation was also used by Abuelyamen *et al.,* [28] on the alpha, beta and gamma types Stirling engines. The performance of the three types engines in terms of power output, thermal efficiency and heat transfer using both similar operational boundary conditions and the same size of the engines was investigated.

Dyson *et al.,* [29] developed for a first time in the U.S. one of the fastest axisymmetric CFD simulation for a free piston Stirling engine. Comparison between the numerical results to those obtained with the use of Sage code shows that the axisymmetric CFD simulation is more accurate than Sage code results. An additional simulation of free piston Stirling engine was performed in 2008, by Dyson *et al.,* [30] using 3D model instead to axisymmetric 2D model under the same assumptions. They found that the computation time was in between one hour to eight hours to compute the full cycle of a FPSE under the latest advances in computer processors at that time.

It is worth mentioning that the numerical simulation in the case of the kinematic engines, the motion of piston and displacer are specified to each other with the velocity profile by using a dynamic mesh method and User Defined Function (UDF) which allows to define their amplitudes as well as the difference phase. Concerning the simulation of the dynamic type, the dynamic mesh method has also been employed [29, 30], but the piston and displacer motions were considered not affected by the developing thermodynamic solution (without fluid-structure interactions).

Hence, the main objective of this work is to develop a two-dimensional axisymmetric CFD simulation of the entire free piston Stirling engine (FPSE) using the dynamic mesh method and the 6DOF solver to study thoroughly the working process of the engine under different conditions, from initial state to motion and stability. The use of 6DOF solver enable us to solve the problem of fluid-structure interactions between the working gas and the rigid body (Piston and displacer) which was not taken into consideration in the research mentioned above. This solver computes external forces by numerical integration of the working gas pressure and the shear stress over the displacer introducing also the gravitational and the spring forces in order to determine exactly the instantaneous position of both the piston and displacer. The Sunpower B-10B free piston Stirling engine shown in Figure 1 is used in this study as a model to verify and validate the simulation. The CFD simulation is performed by ANSYS FLUENT software.

2. Mathematical Background

Figure 1 depicts schematically the studied free piston Stirling engine (FPSE) as a closed cylinder where both the working piston and displacer are connected with it by springs.

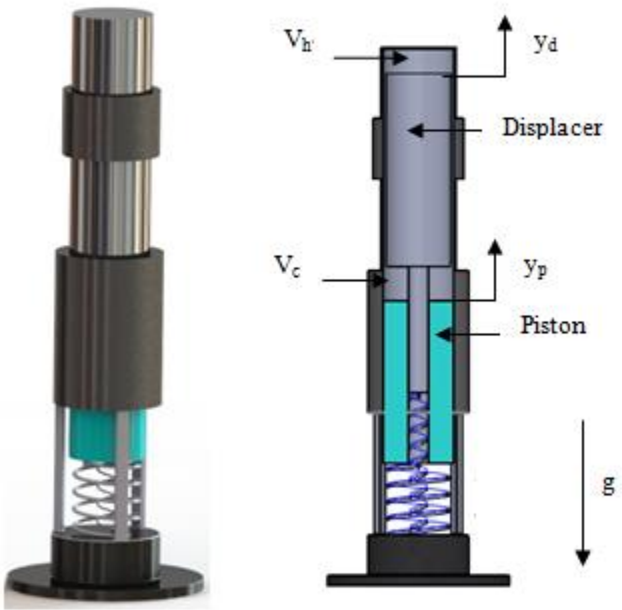

Fig. 1. Schematic of Sunpower B-10B free-piston Stirling demonstrator

The piston and displacer are subjected to the gravity force, spring force, and working fluid pressure force. The following equations of motion are obtained by applying Newton's second law on the FPSE system

$$m_p\ddot{y}_p = -(p - p_{atm})(A_p - A_r) - K_p(y_{p0} + y_p) - m_p g - b_p\dot{y}_p - b(\dot{y}_p - \dot{y}_d) \quad (1)$$

$$m_d\ddot{y}_d = -(p - p_{atm})A_r - K_d(y_{d0} + y_d) - m_d g - b_d\dot{y}_d - b(\dot{y}_d - \dot{y}_p) \quad (2)$$

Considering ($P=P_0$) the engine is in static equilibrium (when the engine is not yet working), equations (1) and (2) can be written as

$$m_p g + k_p y_{p0} = (p_{atm} - p_0)(A_p - A_r) \quad (3)$$

$$m_d g + k_d y_{d0} = (p_{atm} - p_0)A_r \quad (4)$$

with y_{p0} and y_{d0} are respectively the equilibrium positions of piston and displacer. After inserting the equation (3) in eq (1) and eq (4) in eq (2), the equations of motion become

$$m_p\ddot{y}_p = -(p - p_0)(A_p - A_r) - K_p y_p - b_p\dot{y}_p - b(\dot{y}_p - \dot{y}_d) \quad (5)$$

$$m_d\ddot{y}_d = -(p - p_0)A_r - K_d y_d - b_d\dot{y}_d - b(\dot{y}_d - \dot{y}_p) \quad (6)$$

Based on the ideal gas law, the instantaneous pressure of the working fluid can be written as

$$p = m_t R \left[\frac{V_c}{T_c} + \frac{V_h}{T_h} + \frac{V_r}{T_r} \right]^{-1} \tag{7}$$

The variation of volume in the expansion chamber is related only to the motion of displacer, whereas, in the compression chamber, it is related to the motion of both the piston and displacer

$$V_h = V_{h0} - A_d y_d \tag{8}$$

$$V_c = V_{c0} - (A_p - A_r) y_p + (A_d - A_r) y_d \tag{9}$$

The work produced by the FPSE in one thermodynamic cycle can be expressed by the following relation

$$w = \oint p.A_p.dy_p \tag{10}$$

3. Numerical Modelling Approach

The instantaneous position of both the piston and displacer depends on the gravity force, the spring force, the instantaneous working fluid pressure force, and the viscous friction force. The parameters used to measure the instantaneous pressure and viscous forces are determined at each point of space and time based on the Navier-Stokes equations using the Realizable k-ε turbulence model. To solve the pressure–velocity coupling, The SIMPLE algorithm is adopted, and to obtain the best results possible, a second order upwind scheme is used for pressure, density, momentum, energy and turbulence equations.

The numerical model is carried out by ANSYS FLUENT software. This program is based on the finite element method. In order to reduce the computing time, a simplified 2D axisymmetric model is used as an engine geometry. And to provides the best performance and results, the structured quadrilateral mesh with high quality is created in the computational domain which is refined progressively near the walls to form a boundary layer mesh. Number of nodes is 9520 and number of elements is 8886. The calculation domain is shown in Figure 2.

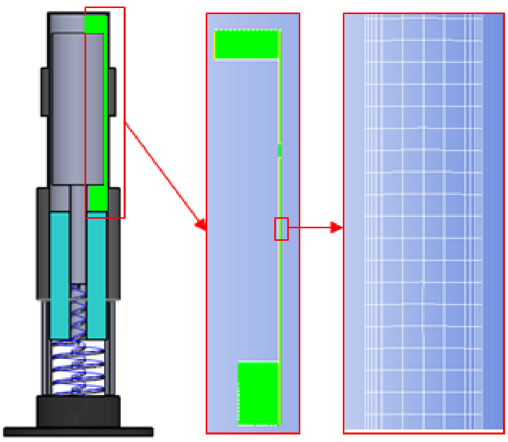

Fig. 2. The scheme of the axisymmetric model and the computational mesh

The natural motion of both the piston and displacer under the effect of the change in the instantaneous working fluid pressure and other forces is achieved via User Define Function (UDF) files, named 6DOF (Six Degrees Of Freedom) programmed in C by introducing the equations of motion mentioned previously. This technique solves the interaction problems between the fluid and rigid bodies [31]. As the piston and displacer move up and down, the 6DOF properties is reduced to a 1DOF model to keep them moving only in a vertical direction. In order to obtain accurate results, 80 iterations per time step are required. The residual for all equations (continuity, energy, and the two momentum equations) is less than 10^{-6}. The numerical solution is carried out using a time step of 10^{-4}s.

Table 1 gives the geometric and physical parameters of the FPSE (Sunpower B-10B). The working fluid used is assumed to be ideal. As the temperature inside the engine varies between 300 (cold heat source) and 600K (hot heat source) the thermal conductivity, dynamic viscosity and specific heat are function of the temperature which is more realistic than using constant values

$$\lambda = 1.5207\times10^{-11}T^3 - 4.857\times10^{-8}T^2 + 1.0184\times10^{-4}T - 3.9333\times10^{-4} \tag{11}$$

$$\mu = 8.8848\times10^{-15}T^3 - 3.2398\times10^{-11}T^2 + 6.2657\times10^{-8}T + 2.3543\times10^{-6} \tag{12}$$

$$C_p = 1.9327\times10^{-10}T^4 - 7.9999\times10^{-7}T^3 + 1.1407\times10^{-3}T^2 - 4.4890\times10^{-1}T + 1.0575\times10^{3} \tag{13}$$

Table 1
Geometric and physical parameters of FPSE [32]

Parameter	Value	Parameter	Value
A_p	1.01e-3 (m^2)	P_{atm}	101325 (pa)
A_d	9.0792 x 10^{-4} (m^2)	V_{h0}	8.567 x 10^{-6} (m^3)
A_r	1.26677 x 10^{-4} (m^2)	V_{c0}	16.036 x 10^{-6} (m^3)
m_p	0.5295 (kg)	T_h	600 (K)
m_d	0.0867 (kg)	T_c	300 (K)

4. Results and Discussion

To simulate the real behavior of the Stirling engine, the investigation is divided into two parts.

4.1 Static State

The working fluid temperature is the same as the ambient temperature and stills constant in both the compression and expansion chambers of the engine. Figure 3 show the variation of the pressure and displacements (y_p and y_d) with a time. It can be seen from this figure the damped motion of piston and displacer from their initial state (t = 0s, $y_p = y_d = 0$ & $p = p_{atm}$) to the equilibrium state under the effect of their weight (gravity force). The moving of the piston to a lower position produce a decrease in pressure in the engine chambers which leads to a new pressure value ensuring the equilibrium.

To check The validity of this simulation, the obtained results are compared with the experimental results published by Martinez Saturno [32] as show in Table 2. It can be seen that the results are not only consistent with the experimental measurements but they are also very approach to the calculations performed numerically on the nonlinear equation system (3 and 4) by using iterative method.

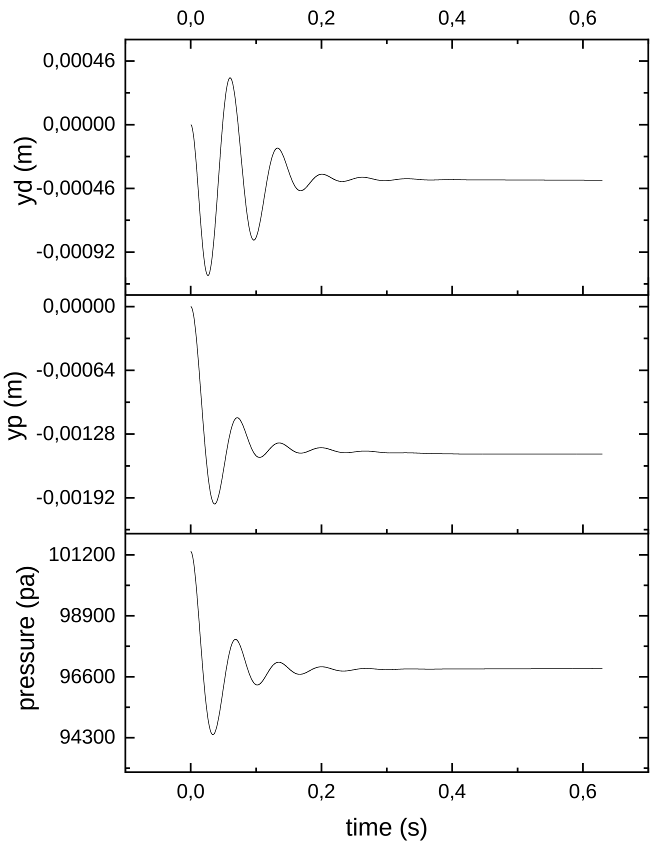

Fig. 3. Pressure and displacement parameters in static state

Table 2
Comparison between the obtained results

Pressure and displacement	Simulation results	Mathematical results	Experimental results [32]
P_0 (pa)	96908,5703	96937	/
y_{p0} (m)	-0.00148	-0.0015	-0.0013
y_{d0} (m)	$-4,01x\ 10^{-4}$	-4.09×10^{-4}	-5.3×10^{-4}

4.2 Dynamic State

This type of Stirling engine is very sensitive. When it is in contact with the hot source, it begins to move gradually [33]. The increase of the temperature in the expansion chamber results in a progressive increase in pressure leading to a disequilibrium of forces. The UDF 6DOF enable both the piston and displacer to function automatically due to the inequality of forces exerted on them. The engine starts to move gradually until it reaches the steady-state oscillations at the 5^{th} second. The variations of the pressure and displacements with time are illustrated in Figure 4.

Figure 5 shows the displacements of the piston and the displacer as a function with time for one cycle. It can be shown that the motion of piston and displacer over one cycle knowing that they both have the same frequency (77.43 rad/s) with different amplitudes 0.0053 m and 0.0064 m respectively, and the phase difference between them is 60.81 degrees. The practical (P-V) diagram is plotted in Figure 6, through which the output work is obtained using a numerical integration which equals 0.13 J and whose output power is 1.6 W.

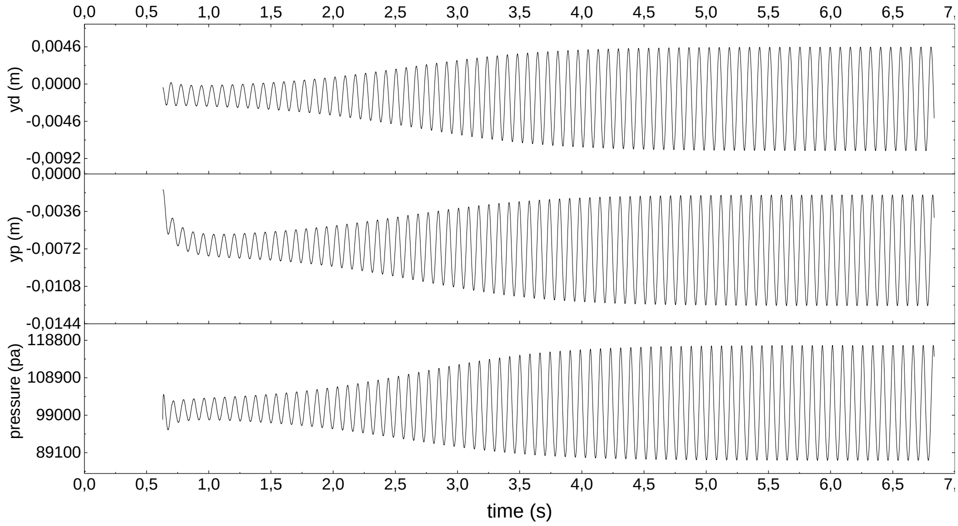

Fig. 4. Pressure and displacement parameters in dynamic state

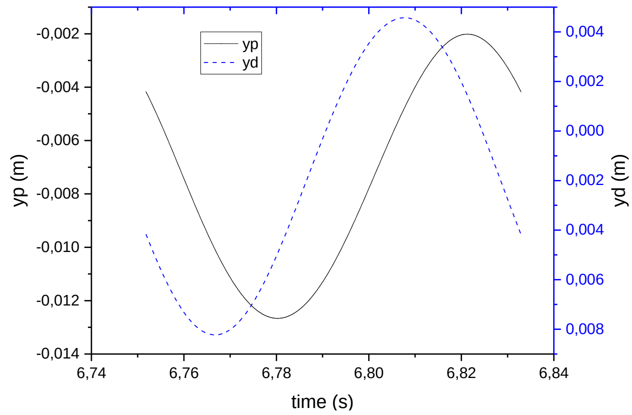

Fig. 5. Displacements of piston and displacer during one cycle (steady state oscillations)

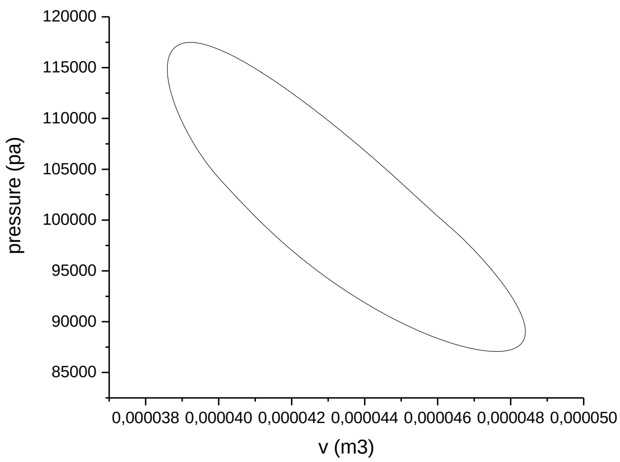

Fig. 6. P-V diagram of the considered FPSE obtained from simulation

5. Conclusion

This work presents a complete simulation of a free piston Stirling engine (FPSE) carried out by using Ansys Fluent coupled with 6DOF solver. This type of investigation describes more thoroughly the working process of engine by taking into account all the different types of forces and physical phenomena occurring in the engine. Moreover, the use of 6DOF in this analysis serves as a technique for determining with accuracy the instantaneous positions of piston and displacer. The results of the first comparison to experimental values of Martinez Saturno [32] realized on the engine of Sunpower B-10B, and those obtained by the resolution of the nonlinear equations of the mechanical system of the engine, show that the physical behavior of the engine can be well predicted. And feasibility of using this method on free piston Stirling engines to estimate the engine's performance. This method provides the first tracks for a more complete modeling of the FPSE operation, that will certainly help in the future to provide answers to the development of the Stirling engine, and the right choice of geometric and physical parameters.

Acknowledgement
The authors would like to express their gratitude to Prof Pascal Stouffs (Université de Pau et des Pays de l'Adour | UPPA) for his help and advice that have given us clear perception of various aspects of Stirling engine. The modeling was performed in the Laboratory LMP2M (Medea University). A special thanks go to Prof Abdellah El Hadj Abdellah for his assistance.

References

[1] Affandi, Rosnani, Zamali Omar, and Mohd Ruddin Ab Ghani. "Feasibility of 25kw Parabolic Dish-Stirling Engine Based Concentrating Solar Power under Malaysia Environment." *International Journal of Engineering & Technology* 7, no. 4 (2018): 3874-3878.
[2] Yatim, Ardiyansyah, Ade Luthfi, and Raden Chemilo. "Biogas-fuelled Stirling engine for electric power generation." In *E3S Web of Conferences*, vol. 67, p. 02015. EDP Sciences, 2018.
[3] Dai, D. D., F. Yuan, R. Long, Z. C. Liu, and W. Liu. "Imperfect regeneration analysis of Stirling engine caused by temperature differences in regenerator." *Energy Conversion and Management* 158 (2018): 60-69.
[4] M. F. Hamid, M. Y. Idroas and Z. A. Zainal. "Preliminary Investigation of an Alpha V-Type Stirling Cooler Development." *Journal of Advanced Research in Fluid Mechanics and Thermal Sciences,* no. 1 (2015): 17-28.
[5] Zare, S. H., A. R. Tavakolpour-Saleh, and O. Aghajanzadeh. "An investigation on the effects of gas pressure drop in heat exchangers on dynamics of a free piston Stirling engine." *International Journal of Engineering-Transactions B: Applications* 30, no. 2 (2017): 150-160.
[6] Sim, Kyuho, and Dong-Jun Kim. "Identification of Damping Characteristics of Free-piston Stirling Engines via Nonlinear Dynamic Model Predictions." *Transactions of the Korean Society for Noise and Vibration Engineering* 26, no. 3 (2016): 248-257.
[7] Batmaz, Ihsan, and Süleyman Üstün. "Design and manufacturing of a V-type Stirling engine with double heaters." *Applied Energy* 85, no. 11 (2008): 1041-1049..
[8] Senft, James R., and J. R. Senft. *Ringbom stirling engines*. Vol. 200. New York: Oxford university press, 1993.
[9] Walker, Graham, G. Reader, O. R. Fauvel, and Edward R. Bingham. "The Stirling alternative. Power systems, refrigerants and heat pumps." (1993).
[10] Dyson, Rodger, Scottt Wilson, and Roy Tew. "Review of computational stirling analysis methods." In *2nd International Energy Conversion Engineering Conference*, p. 5582. 2004.
[11] Walker, G. *Stirling-Cycle Engines.* Clarendon Press, 1973.
[12] Urieli, Israel, and David M. Berchowitz. *Stirling cycle engine analysis*. Bristol: A. Hilger, 1984.
[13] Cullen, Barry, and Jim McGovern. "Energy system feasibility study of an Otto cycle/Stirling cycle hybrid automotive engine." *Energy* 35, no. 2 (2010): 1017-1023.
[14] Tavakolpour-Saleh, A. R., S. H. Zare, and H. Bahreman. "A novel active free piston Stirling engine: Modeling, development, and experiment." *Applied energy* 199 (2017): 400-415.
[15] Finkelstein, Theodor. "Insights into the thermodynamics of Stirling cycle machines." In *Intersociety Energy Conversion Engineering Conference*, p. 3951. 1994.

[16] Parlak, Nezaket, Andreas Wagner, Michael Elsner, and Hakan S. Soyhan. "Thermodynamic analysis of a gamma type Stirling engine in non-ideal adiabatic conditions." *Renewable Energy*34, no. 1 (2009): 266-273.
[17] Martini, W. R. "Stirling Engine design manual second edition." *Technical report, NASA CR 168088* (1983).
[18] Cheng, Chin-Hsiang, and Ying-Ju Yu. "Numerical model for predicting thermodynamic cycle and thermal efficiency of a beta-type Stirling engine with rhombic-drive mechanism." *Renewable Energy* 35, no. 11 (2010): 2590-2601.
[19] Mehdizadeh, Nasser Seraj, and Pascal Stouffs. "Simulation of a martini displacer free piston stirling engine for electric power generation." *International Journal of Thermodynamics* 3, no. 1 (2000): 27-34.
[20] Urieli, Israel, Costa J. Rallis, and David M. Berchowitz. "Computer simulation of Stirling cycle machines." In *12th intersociety energy conversion engineering conference*, pp. 1512-1521. 1977.
[21] Finkelstein, T. "Computer analysis of Stirling engines." In *Advances in Cryogenic Engineering. Volume 20*, vol. 20, pp. 269-282. 1975.
[22] Tew, Roy C., Kent Jefferies, and David Miao. *A Stirling engine computer model for performance calculations*. Vol. 78884. Department of Energy, Office of Conservation and Solar Applications, Division of Transportation Energy Conservation, 1978.
[23] Organ, A. J. "Gas dynamics of the temperature-determined Stirling cycle." *Journal of Mechanical Engineering Science* 23, no. 4 (1981): 207-216.
[24] Gedeon, David. "Sage-Object-oriented software for Stirling machine design." In *Intersociety Energy Conversion Engineering Conference*, p. 4106. 1994.
[25] Mahkamov, K. "An axisymmetric computational fluid dynamics approach to the analysis of the working process of a solar Stirling engine." *Journal of solar energy engineering* 128, no. 1 (2006): 45-53.
[26] Mahkamov, K. "Design improvements to a biomass Stirling engine using mathematical analysis and 3D CFD modeling." *Journal of Energy Resources Technology* 128, no. 3 (2006): 203-215.
[27] Li, Zhigang, Yoshihiko Haramura, Yohei Kato, and Dawei Tang. "Analysis of a high performance model Stirling engine with compact porous-sheets heat exchangers." *Energy* 64 (2014): 31-43.
[28] Abuelyamen, Ahmed, and Rached Ben-Mansour. "Energy efficiency comparison of Stirling engine types (α, β, and γ) using detailed CFD modeling." *International Journal of Thermal Sciences* 132 (2018): 411-423.
[29] Dyson, Rodger, Scott Wilson, Roy Tew, and Rikako Demko. "Fast whole-engine Stirling analysis." In *3rd International Energy Conversion Engineering Conference*, p. 5558. 2005.
[30] Dyson, Rodger W., Steven M. Geng, Roy C. Tew, and Miguel Adelino. "Towards fully three-dimensional virtual Stirling convertors for multi-physics analysis and optimization." *Engineering Applications of Computational Fluid Mechanics* 2, no. 1 (2008): 95-118.
[31] Fluent, A. N. S. Y. S. "12.0 User's Guide, 2009." *Fluent Inc., New Hampshire*.
[32] Martinez Saturno, Jose Gregorio. "Some mathematical models to describe the dynamic behavior of the B-10 free-piston Stirling engine." PhD diss., Ohio University, 1994.
[33] Redlich, R. W., and D. M. Berchowitz. "Linear dynamics of free-piston Stirling engines." *Proceedings of the Institution of Mechanical Engineers, Part A: Power and process engineering* 199, no. 3 (1985): 203-213.